Bending behaviour of thin-walled perforated channel beams with modified cross-sectional shape – Part 1: experimental tests and FSM

Piotr PACZOS[ID], Aleksandra M. PAWLAK[ID]*, Paweł JASION[ID], and Michał PLUST[ID]

Poznań University of Technology, Institute of Applied Mechanics, Jana Pawła II 24, 60-965 Poznań, Poland

Abstract. The subject of this study is thin-walled channel sections with a modified cross-sectional shape. The investigation involved six beams, three of which had perforations on the web, while the other three had a flat, solid web. The beams were subjected to four-point bending tests. Experimental tests were conducted using both electronic and optical methods, with a test setup specifically designed for this investigation. Additionally, numerical analyses were performed using the finite strip method. The primary objective of the research was to determine the impact of web perforations on the strength and stability of the bent beams. The perforation of the web also resulted in a reduction in the overall weight of the structure, thereby decreasing material consumption. Based on the research, the critical forces and maximum forces at which total loss of load-bearing capacity occurred were determined. Furthermore, the buckling modes of the beams were identified. The study revealed that the critical and maximum forces for beams with perforated webs were lower compared to beams with a flat, solid web. However, the significant reduction in weight for the perforated beams suggests that their use remains advantageous. The results of FEM and analytical analyses, essential for modelling and understanding complex behaviours in thin-walled structures, will be presented in the second part of this publication to maintain clarity and accessibility.

Keywords: thin-walled channel beams; web perforations; four-point bending; structural stability; buckling analysis.

1. INTRODUCTION

Thin-walled structures made by cold-forming technology are a popular structural element in civil engineering structures, in the transportation industry, such as the automotive or railroad industries, as well as in the space industry. Nowadays, the aim is to reduce the amount of material input in the manufacture of particular products, and this requirement is met by thin-walled structures which, with their low weight and low material intensity, are high-strength. In addition, thin-walled structures formed by cold-forming technology are simple to assemble.

Today, an example of attained additional reinforcement of thin-walled cold-formed structures is the adherence of carbon-fibre polymer tapes (so-called CFRP tapes). Pawlak et al. [1] prepared a comprehensive review of current solutions related to the strengthening of structures using CFRP tapes. The authors also presented the disadvantages, advantages, and risks of this method of strengthening thin-walled structures. In addition, Pawlak and Paczos [2] highlighted the strengthening of cold-formed thin-walled structures by introducing additional bends in the cross-section of compressed columns. Shahbazian and Wang [3] conducted a theoretical analysis of channels having single, double, or triple v-shaped bends on the web. Li and Young [4] performed a bending test on sections with single v-shaped modifications in the cross-section. They connected the

sections with sheet metal screws. As a result of joining two channel sections, they obtained an open I-section and a closed rectangular section. Zhang and Alam [5] studied the compression behaviour of channels having single bends on the web and perforations. Modified cross-sectional shapes are also described in [6,7]. Many scientists and researchers analyze classical cross-section shapes such as lipped channels [8–12]. In the present study, channel sections with a modified cross-sectional shape were analyzed, with the flange of one of the sections shaped as trapezoids. In addition, sections with perforations on the web were examined. The classic channel-shaped lipped channel was also examined.

In the present study, the beams were subjected to a four-point bending test. For this purpose, a special stand was prepared to ensure that a constant bending moment occurs between the supports of the beam. For thin-walled sections with perforations on the web or flange, it is difficult to avoid the occurrence of flexural-torsional buckling, as reported by Khazaal et al. [13] and Yu et al. [14]. Numerous researchers and scientists described the occurrence of this phenomenon in their work, including Rajkannu and Jayachandran [15], Muteb and AL-Shareef [16], and Visy et al. [17]. This is because to obtain pure bending conditions, it is necessary to apply a bending force at the shear centre of the beam cross-section, which is usually, geometrically, outside the cross-section. Thus, the application of a force at a point where the beam flange is physically absent is an issue that is difficult to implement in reality. In addition, to avoid the appearance of the flexural-torsional buckling effect, stiffeners can be used. In the beam, special diaphragms are placed at the

*e-mail: aleksandra.pawlak@put.poznan.pl

support locations and the point of force application, as shown by Wang *et al*. [18]. The four-point bending test is described by Yu *et al*. [19]. The subjects of the study were channel sections having perforations on the web.

As mentioned previously, for the experimental studies presented in this paper, a special test stand was designed and fabricated to avoid the occurrence of flexural-torsional buckling and to allow pure bending conditions. This entire process is described in the paper [20]. This paper describes the experimental tests conducted using the strain gauge method and the optical method. Six beams were tested, including three without web perforations and three with web perforations.

The paper also shows numerical analyses conducted using the finite strip method (FSM). The FSM method does not allow analysis of beams that have perforations on the web, and for this reason, only three beams were numerically tested. Huang *et al*. [21] analyzed channel beams having reinforcement in the form of ribbing in the web. The beams they tested were subjected to bending and they used the FSM method. Grenda and Paczos [22] presented experimental tests and FSM analyses of bent beams with a modified cross-sectional shape. Szymczak and Kujawa [23] applied the FSM method to the analysis of compression channel beams with a standard cross-sectional shape made by lamination technology.

Additionally, advanced techniques for crack detection and propagation modelling, including the cracking elements method for quasi-brittle fracture [24, 26], and wavelet-based approaches for early crack revealing [25], were proposed in recent works. Although they do not focus directly on thin-walled cold-formed structures, these methodologies offer valuable insights into failure mechanisms and can perform the analysis of structural elements with perforations or complex geometries.

The above literature review proves that experimental methods (strain gauge and optical) and numerical analysis of FSMs find their application in the study of thin-walled sections made by cold-forming technology. In addition, it was pointed out that few researchers and scientists are engaged in the analysis of sections with a high degree of cross-sectional shape modification. Cross-sectional shape modifications have a favourable effect on the weight-to-strength ratio or resistance to loss of stability of thin-walled sections. The analysis of thin-walled structures, even those with classical cross sections, poses many difficulties. Modifying cross-sectional shapes generates many questions and many issues that still require research and analysis.

This article introduces significant innovations in the analysis of structures with modified cross-sectional shapes, specifically focusing on trapezoidal flanges. Unlike existing literature that predominantly examines standard cross-sectional shapes, such as lipped channels, this work explores the potential benefits of these modified shapes in structural optimization. Furthermore, the research addresses the pressing need for lightweight constructions with minimal material consumption by investigating the effects of perforation in the web of beams. The findings aim to enhance the understanding of how these innovative modifications can improve the stability and load-bearing capacity of structures, thus contributing valuable insights to the field of structural engineering.

2. GEOMETRY OF CROSS SECTIONS AND MATERIAL PROPERTIES

This study focuses on six thin-walled cold-formed channel beams (designated as B1, B2, B3, B4, B5, and B6) with modified cross-sectional shapes. Among these beams, three have solid webs (B1, B3, and B5), while the remaining three feature perforated webs (B2, B4, and B6). The dimensions of the beam cross sections are detailed in Fig. 1 and Table 1.
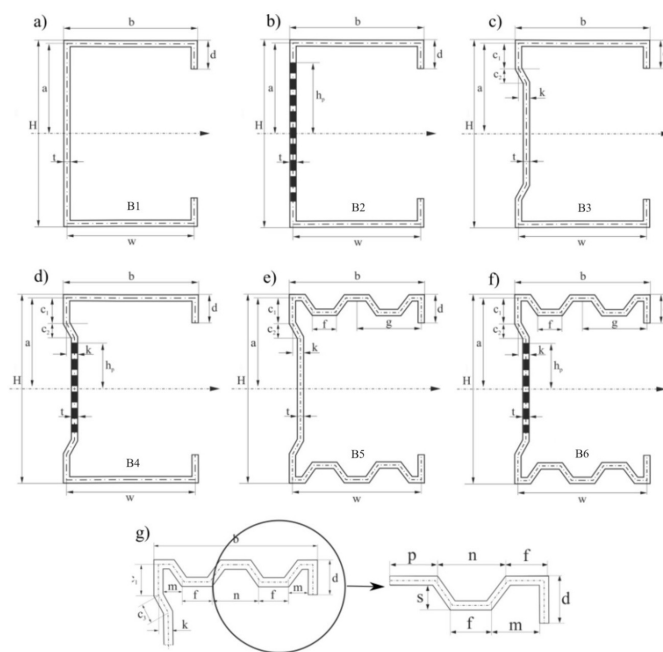

Fig. 1. Dimensioned cross-sections of the analyzed beams

Table 1

Dimensions of the cross-sections of the beams

H	=	160.0 mm	c_1	=	18.0 mm
b	=	80.0 mm	c_2	=	10.0 mm
a	=	79.5 mm	c_3	=	10.0 mm
w	=	79.0 mm	f	=	10.0 mm
d	=	18.0 mm	g	=	36.0 mm
h_{p2}	=	68.5 mm	n	=	24.0 mm
$h_{p4,6}$	=	40.0 mm	m	=	18.0 mm
k	=	8.0 mm	s	=	15.0 mm

Figure 2 shows the dimensions of the perforations and a picture of the web of a beam with perforations. The shape and arrangement of the pattern are determined by the technological capabilities of the company that manufactured the profiles.

The perforation takes the form of small holes (Fig. 2), whose diameter is $d_1 = 5$ mm. The distance between the holes is $p_1 = 3$ mm. The height of the perforation of beam B2 was denoted as h_{p2}, and the perforation height of beams B4 and B6 was $h_{p4,6}$. This perforation pattern is designed to reduce the overall weight of the structure. The study will evaluate the
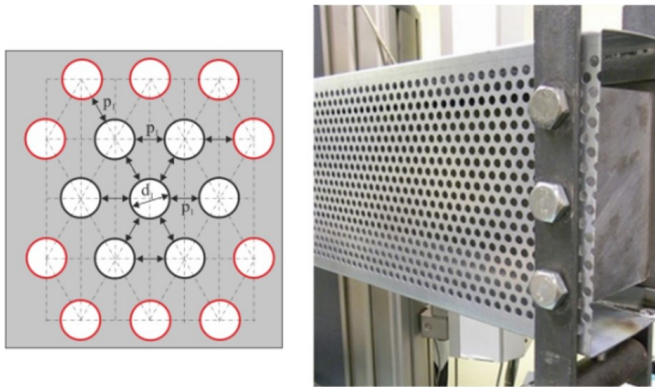
2

Bull. Pol. Acad. Sci. Tech. Sci., vol. 73, no. 3, p. e153830, 2025

Fig. 2. Geometry and dimension of perforations

impact of these perforations on the strength and stability of the beams.

The sheets of metal beams were tested with three different thicknesses $t = 0.6$, 1.0, 1.4 mm and four different lengths $L = 400$, 500, 600 and 800 mm. The beams were made of cold-rolled DX51 sheets. A static tensile test was performed on samples cut from the sheet from which the beams were made. The tensile test was performed according to the procedures contained in EN 10002-1:2001. The purpose of these tests was to determine the mechanical properties of the material from which the beams were made. Eight specimens were prepared for the tensile test – four were cut parallel to the rolling direction of the sheet, and four were cut perpendicular to the rolling direction. The resulting stress-strain graphs from the static tensile test are presented in Fig. 3.
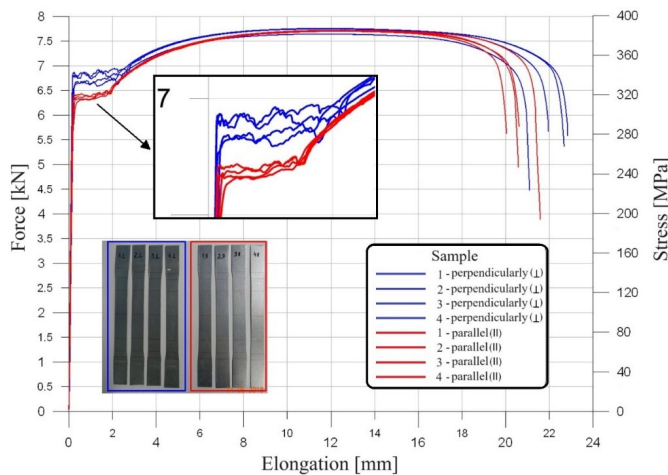

Fig. 3. Force as a function of sample elongation – static tensile test results

From the static tensile test, the values of Young's modulus E, upper yield strength R_{eH}, tensile strength R_m were determined, and the value of Poisson's coefficient ν was determined. The results obtained from the tensile test are shown in Table 2.

The mechanical properties of the steel from which the beams were made were implemented in the programme in which the finite strip analysis was performed.

Table 2
Mechanical properties of DX51 steel obtained from static tensile test

Parameter	Symbol	Value	Unite
Young's modulus	E	185	[GPa]
Upper yield strength	R_{eH}	328	[MPa]
Tensile strength	R_m	396	[MPa]
Poisson's ratio	ν	0.3	[–]

3. EXPERIMENTAL RESEARCH

The samples used for the experimental tests were manufactured by the Polish company "Zaprom" [27]. The company "Zaprom" implemented a project titled "Establishment of a Research and Development Center and Conducting Industrial Research Focused on Optimizing Thin-Walled Sheet Metal Structural Elements and Developing Efficient Manufacturing Technologies." The project aimed to enhance the company's competitiveness by establishing an R&D Center specializing in optimizing sheet metal structures and developing efficient technologies for their production, thereby increasing the facility's expertise in specialized sheet metal processing machinery.

The project focuses on developing open-profile structures with high technical parameters while ensuring they can be produced on efficient, automated roll-forming lines. Figure 4 shows the optimized profiles developed during the project, and the profiles discussed in this study were made possible thanks to the technologies developed as part of this project.
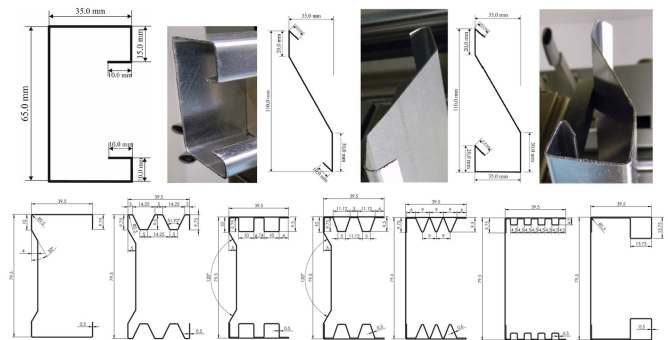

Fig. 4. The modified cross-sectional shapes produced by the company Zaprom

The primary objective of these experimental tests was to validate the results obtained through the CuFSM numerical method. The beams subjected to these tests are depicted in Fig. 5. They were fabricated from sheet metal, with the mechanical properties detailed in Fig. 3 and Table 2.

Experimental tests were conducted using a ZWICK Z100 universal testing machine, with a measurement range of 0.2 to 100 kN. The applied loading on the beams and the data collected from the strain gauges were recorded digitally. To ensure pure bending conditions, a custom test stand was designed and constructed, as illustrated schematically in Fig. 6. This setup provided a constant bending moment along the length
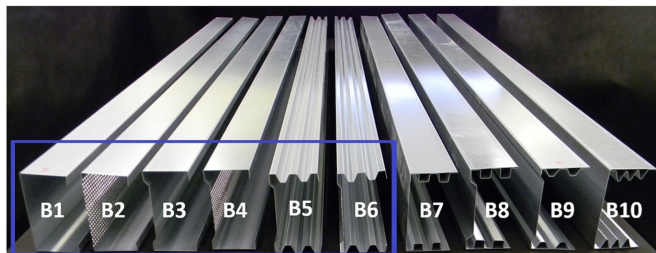
Bull. Pol. Acad. Sci. Tech. Sci., vol. 73, no. 3, p. e153830, 2025

3

P. Paczos, A.M. Pawlak, P. Jasion, and M. Plust

Fig. 5. Beams that were subjected to experimental testing (circled in blue)

Fig. 6. Schematic of test stand

Fig. 7. The beam, gauge, and experimental test stand (beam B3)

lize the digital image correlation (DIC) method. This technique involves scanning the surfaces of the beams, which were pre-coated with a black-and-white pattern to enable the scanner to accurately detect reference points across the entire surface. Strains and displacements were continuously recorded in real time. The ARAMIS system measures displacements with an accuracy of up to 0.01 mm. The load force applied to the beam was measured using a load cell integrated into the ZWICK Z100 machine. The deformation measurements were out-of-plane, which indicates the direction of the measurements. The results are presented as a series of images captured over short intervals, which, when compiled, create a film that allows for the observation of beam deformations even after the completion of the tests.

Analyzing stability loss is a complex challenge. Optical methods, which offer comprehensive information on strain and displacement across the entire beam surface, facilitate more accurate analysis compared to traditional strain gauge testing. Strain gauges measure strain only at specific points where they are attached, whereas optical methods provide a broader and more reliable view of strain and displacement. This advantage makes optical methods particularly valuable for understanding the buckling and failure mechanisms of cold-formed thin-walled beams, especially those with modified cross-sectional shapes. Figure 8 illustrates the force versus deflection curves for beams subjected to pure bending, alongside results from the optical measurements. The optical data reveal characteristic half-waves of local buckling observed on the webs of the bent beams.

Beams B5 and B6, due to their stiffened webs, exhibited distortional buckling, where the entire cross-section (both flanges and web) rotated. No half-waves were observed in the compressed flange, and the buckling moment was not distinctly visible in the graphs. Figure 9 presents the results of the numerical FEM analysis, as well as the experimental and optical strain

of the beam, which was set to 500 mm for the experimental tests.

The stand used for the tests, along with the deflection sensors and location of the strain gauges, is shown in Fig. 7.

The following equipment was used for experimental investigations: strain gauge bridge Spider electronic measuring system, the deflection sensor 10 mm (WI10) Hotinger, foil strain gauges HBM type 6/120LY11: resistance 120 W ±0.35%, gauge factor 2. The shape of the cross-section of a beam, equipment, and experimental test stand are presented in Fig. 6. In addition to strain gauges, an optical measuring system was simultaneously used to measure beam deflection and strain.

Optical measurements were conducted during the tests, providing detailed insights into the displacements and strains across the entire bent beam. This method primarily facilitated the determination of beam buckling modes. The optical testing was performed using the ATOS and ARAMIS systems, which uti-
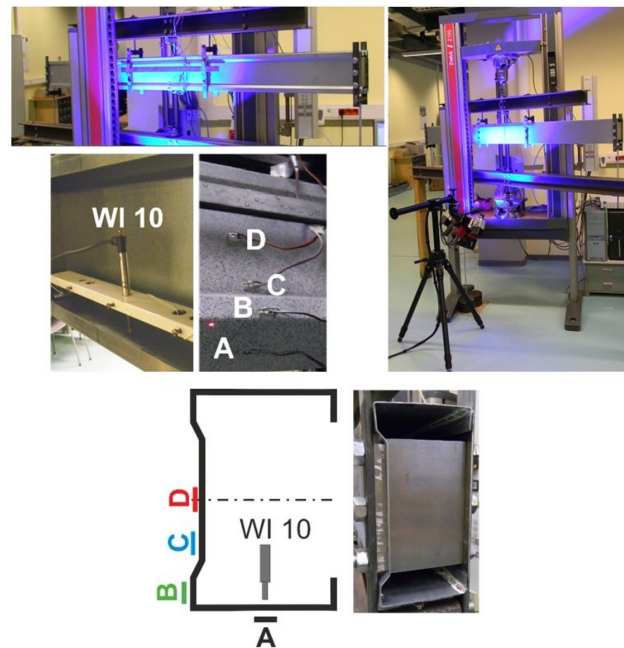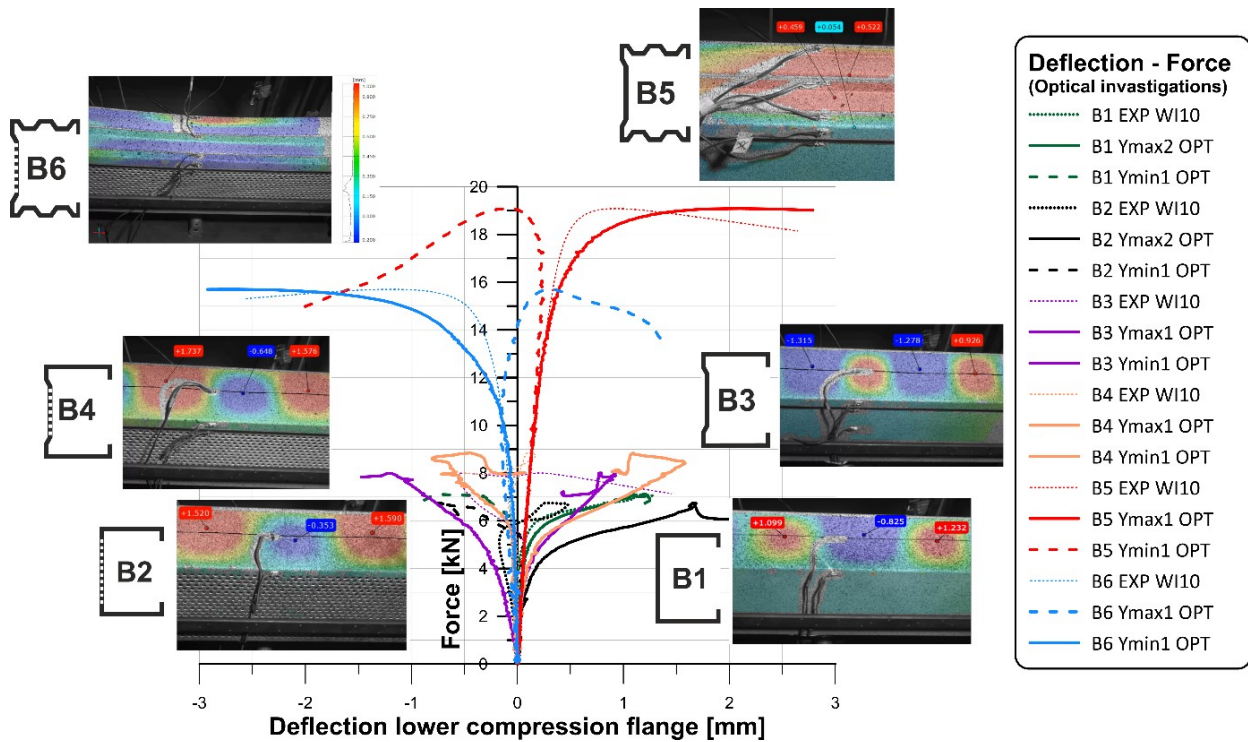
4

Bull. Pol. Acad. Sci. Tech. Sci., vol. 73, no. 3, p. e153830, 2025

Bending behaviour of thin-walled perforated channel beams with modified cross-sectional shape – Part 1

Fig. 8. Deflection compression flange vs. force (Beams: B1–B6) – experimental optical tests

measurements for beam B5. The experimental and optical results are summarized in Table 3. Additionally, the FEM analysis was described in detail in the second part of this work.
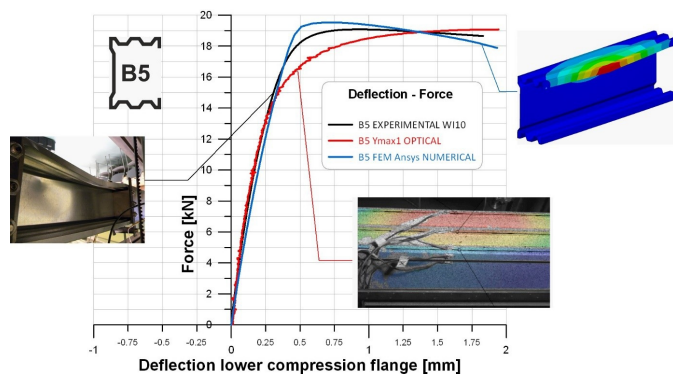

Fig. 9. Deflection compression flange vs. force – comparison of the results of numerical, experimental classical and optical tests

The critical force values for the experimentally tested columns were determined using both the strain-averaged method and the tangent method. The choice of method was based on the shape of the force-strain diagram. In some cases, the more accurate strain-averaged method could not be applied. This method involves dividing the force-strain curve into buckling and post-buckling regions. Each region is then approximated linearly, and the intersection of these lines indicates the critical force value.

The graphs in Fig. 10 present average strain values from the strain gauges placed on the compressed sections of the beams,

plotted against the applied force. To determine the critical force for beams B1 and B3, the method of average strain was applied, identifying the linear pre-buckling and nonlinear post-buckling regions on the graph. Linear approximations of these regions
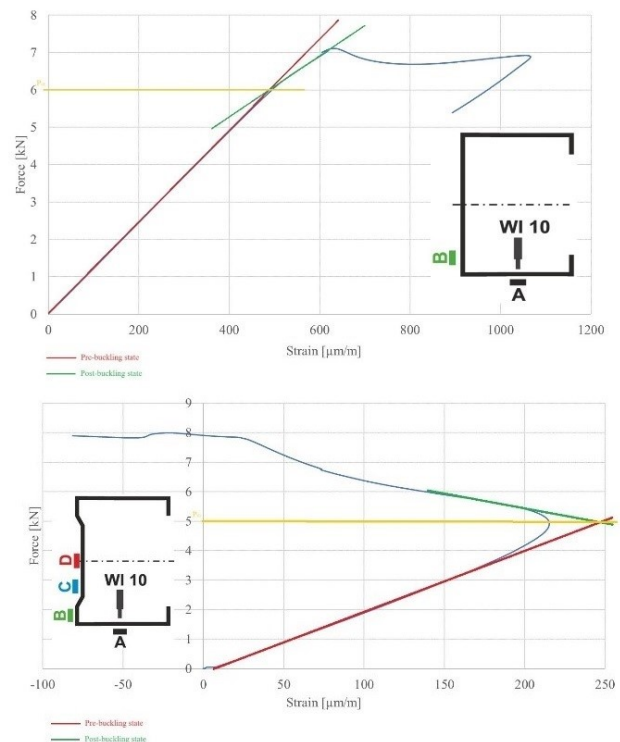

Fig. 10. Determination of the critical force by averaged strain method

were used to find the critical force at the intersection point of the two lines. The yellow line marks this intersection and projects the critical force onto the force axis.

In the case of beam B5, due to the specific shape of the load-displacement curve, the critical force was determined using the tangent method (Fig. 11), which is more suitable for this case. This method approximates the pre-buckling linear region and identifies the critical force as the point where the linear approximation no longer aligns with the curve. The yellow line on the graph marks this divergence by projecting the critical point onto the force axis, allowing for the accurate identification of the critical force.
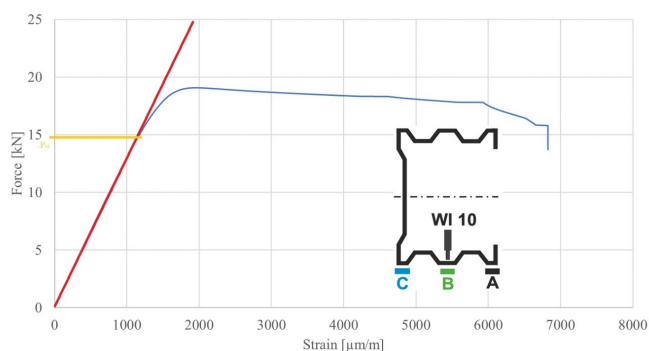

Fig. 11. Determination of the critical force using the tangent method

Table 3 shows the values of the critical forces obtained and the maximum forces at which the beams completely lost their load-bearing capacity. The weights of all the tested beams are also indicated.

Table 3

The results of experimental investigation (weight, critical, and maximum force)

Beams	Weight [kg]	Critical force [kN]	Maximum force [kN]
B1	5.16	6.0 (local)	7.07
B2	4.40	5.1 (local)	6.73
B3	5.25	5.0 (local)	8.00
B4	4.78	6.5 (local)	8.84
B5	6.31	14.9 (distortional)	19.2
B6	5.85	11.2 (distortional)	15.7

4. FINITE STRIP METHOD

Numerical analyses were conducted using CuFSM version 4.03, a program that employs the finite-strip method, an extension of the finite element method. Unlike the finite element method, which divides the sample or element into discrete finite elements, the finite-strip method divides the element into strips. The accuracy of the results depends on the strip discretization, so convergence studies were performed to determine the optimal number of strips for both the flange and the web.

Based on the analyses performed, the critical moments and the contribution of each buckling mode to the overall loss of stability were determined. To conduct the analysis using the finite strip method, it is first necessary to input the relevant data, including the mechanical properties of the material from which the beams are made. These properties, obtained from the static tensile tests described in Section 2, were entered into the program. Subsequently, the cross-sectional shape of the test beams was defined, and the cross-section was divided into strips, accordingly, as illustrated in Fig. 12.
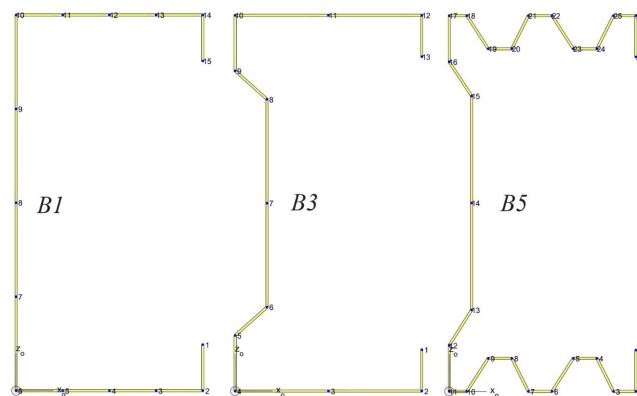

Fig. 12. Determination of cross-sectional shapes and division into strips

Three beams (B1, B3, and B5) were analyzed. These beams have solid, flat webs without perforations. Beams with perforations were excluded from the analysis due to the limitations of the CuFSM v. 4.03 program. A constant load generator was used to apply a bending moment, with boundary conditions and load settings chosen to ensure pure bending conditions. It is important to note that the load and boundary conditions were selected to facilitate a comparison between the results of the finite strip method (FSM) analysis and the experimental tests.

Based on the analyses, the critical moments and the contributions of various buckling modes to the total loss of stability were determined. Figure 13 presents the diagrams obtained and illustrates the shape of the cross-section at the moment of critical load for all analyzed beams.

The result of the FSM analysis is the graph shown above. The program determines the critical force as the first minimum that appears on the graph. The red "data" point allows navigation through the graph and the individual data points, enabling a detailed examination of the results for various buckling wavelengths.

Table 4 presents the contributions of each buckling mode to the total loss of stability. All beams primarily experienced local loss of stability. Notably, beams with more modified cross-sectional shapes exhibited a higher proportion of distortional buckling, a finding corroborated by experimental tests using the optical method. Table 5 provides the critical force values obtained from the finite-strip method. The analysis was conducted on beams without web perforations - specifically, beams B1, B3, and B5. Numerical simulations using the finite strip method were performed on beams with a length of 500 mm, matching the length of the beams used in the experimental study.
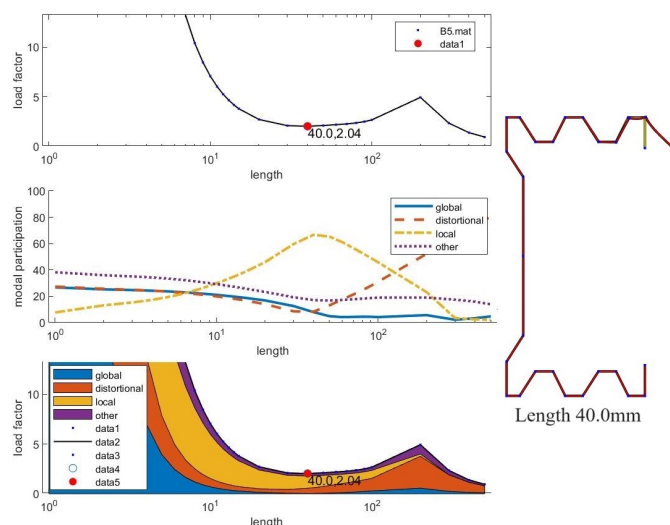
6

Bull. Pol. Acad. Sci. Tech. Sci., vol. 73, no. 3, p. e153830, 2025

Bending behaviour of thin-walled perforated channel beams with modified cross-sectional shape – Part 1
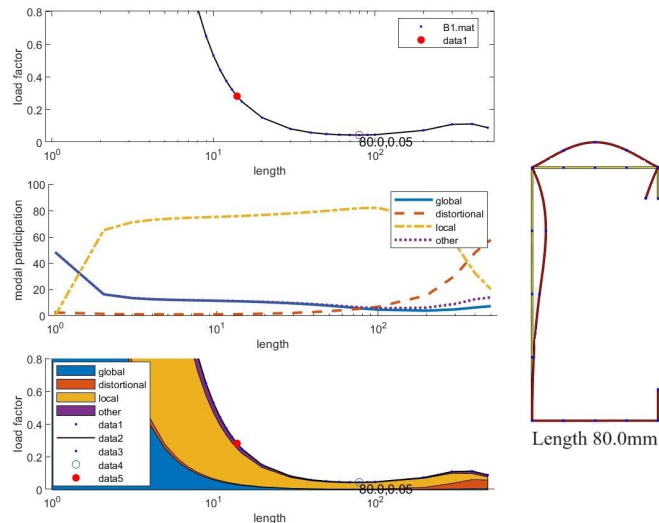
(a) beam B1
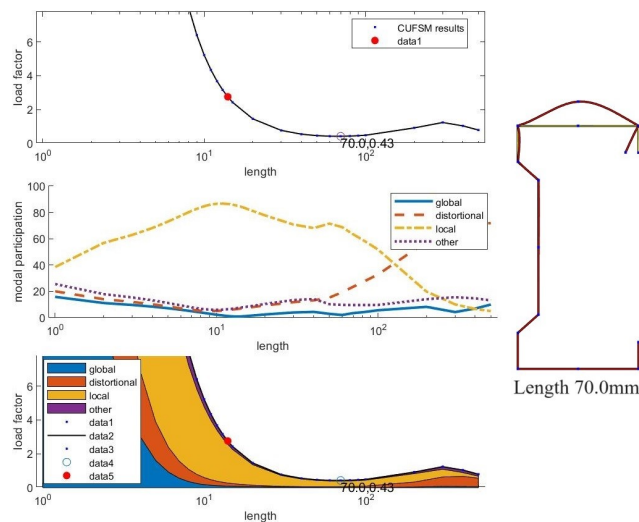
(b) beam B3

(c) beam B5

Fig. 13. Beam length as a function of load factor and the contributions
of each buckling mode to total loss of stability

Table 4
Contribution of individual buckling modes to total loss of stability

Beam	Global	Distortional	Local	Other
B1	0.2%	0.9%	98.7%	0.2%
B3	2.8%	10.9%	78.0%	8.2%
B5	1.7%	25.2%	61.0%	12.1%

The buckling mode labelled "other" indicates the interaction of different buckling forms: global, local, and distortional. This interaction reflects the complex behaviour observed during the tests, where multiple modes contribute to the overall deformation pattern.

Table 5
Results of finite strip analysis

Critical force F_{cr} [kN]			
Beam	B1	B3	B5
Length L [mm]	500		
$t = 1$ mm	5.07	5.67	31.49

Using the finite strip method, the buckling modes of the beams were first determined. The critical force values for beams B1 and B3 were found to be greater than 5 kN. In contrast, the critical force for beam B5 was 31.49 kN, which is significantly higher than the value observed in the experimental study. This substantial discrepancy will be addressed in the conclusion.

5. COMPARISON AND CONCLUSION

Six beams were tested: three with perforated webs and three with solid, flat webs. The objective was to assess how perforations influence the beam weight, strength, and stability. Perforations in thin-walled beams are of particular interest, as they optimize stress distribution, potentially enhancing load-bearing capacity despite material reduction. Additionally, three beams with a flat, solid web were analyzed numerically using the finite strip method. Table 6 provides a summary of the critical and maximum forces at which the beams failed.

Table 6
Critical forces and maximum forces, EXP – experimental tests,
FSM – finite strip method

Beam	$F_{cr_{EXP}}$ [kN]	$F_{max_{EXP}}$ [kN]	$F_{cr_{FSM}}$ [kN]
B1	6.00	7.07	5.07
B2	5.10	6.73	–
B3	5.00	8.00	5.67
B4	6.50	8.84	–
B5	14.90	19.2	31.49
B6	11.20	15.7	–

Bull. Pol. Acad. Sci. Tech. Sci., vol. 73, no. 3, p. e153830, 2025

7

The critical force values for beams with web perforations are generally lower than for those with a solid web. An exception is beam B4, which has a critical force of 6.5 kN, compared to 5.0 kN for beam B3, which has the same cross-sectional shape but a solid web. This indicates that perforations can sometimes enhance beam stiffness by altering stress paths within the structure. The B4 profile is an exception, in which an increase in stiffness and critical load was observed due to the application of perforations. Although initially expected to weaken the profile structure, perforations in B4 facilitate optimized stress distribution, enhancing load-bearing capacity. Consequently, the critical load value for the B4 profile was found to be higher than that of the B3 profile, which is corroborated by the results of the conducted studies.

The B1–B4 columns were subject to local loss of stability, which was found based on experimental tests, and especially on the basis of optical tests. Local loss of stability was observed in beams B1 through B4, confirmed by both experimental and optical tests, which provided real-time displacement data. Numerical analyses corroborated these findings. Beams B5 and B6 exhibited distortional buckling, with beam B5 showing local buckling as the dominant mode and distortional buckling contributing 25.2%. More complex cross-sectional shapes and additional bends correlated with increased distortional buckling. These findings emphasize the impact of cross-sectional modifications on stability modes, a critical consideration in the design of lightweight structures, where managing local buckling and distortional effects is essential.

Table 7 summarizes the impact of beam weight reduction on strength and stability, highlighting the relationship between decreased weight and its effect on performance. The weight of a structure is a fundamental parameter that is easy to measure and plays a crucial role in structural design. Modern designs prioritize lightweight structures and material conservation, making weight reduction highly significant.

Table 7
Nondimensional critical and maximum moments with corresponding beam weights

Beam	Weight [kg]	$F_{\text{cr}_{\text{EXP}}}$ [kN]	$F_{\text{max}_{\text{EXP}}}$ [kN]
B1	5.19	6.0	7.07
B2	4.40	5.1	6.73
B1/B1	1.00	1.00	1.00
B2/B1	0.85	0.85	0.95
B3	5.25	5.0	8.00
B4	4.78	6.5	8.84
B3/B3	1.00	1.00	1.00
B4/B3	0.91	1.30	1.11
B5	6.31	14.9	19.2
B6	5.85	11.2	15.7
B5/B5	1.00	1.00	1.00
B5/B6	0.93	0.75	0.82

To correctly interpret Table 7, it is essential to understand that B1/B1 is the reference value, where 1.0 represents 100%. The other beams are compared to B1, illustrating the differences in their masses. For example, the ratio of the mass of beam B2 to beam B1 (B2/B1) is 0.85, indicating that the mass of beam B2 is 85% of the mass of beam B1; thus, the mass of beam B2 is 25% less than that of beam B1. Based on the above table, it can be concluded that:

- The weight of beam B2 compared to beam B1 decreases by 25%. The critical force for beam B2 is 25% lower than the critical force for beam B1. However, the maximum force for B2 is only 5% lower than for B1.
- For beams B3 and B4, the difference in their weights is 9%. The critical force for beam B4, a beam with perforations, increases by 30% compared to beam B3 (without perforations). For the maximum force, the increase is 11%.
- The weight of beam B5 compared to beam B6 decreases by 7%. The critical force for beam B5 is 35% lower than for beam B5. The maximum force for beam B5 is 18% lower than for beam B6.

For beams B1 and B2, there was a noticeable decrease in critical and maximum force values alongside a significant weight reduction. The same trend was observed for beams B5 and B6. This relationship between weight and force capacity, visualized in Fig. 14, underscores the trade-offs in designing lightweight structures and the necessity to balance weight reduction against reduced force capacities.
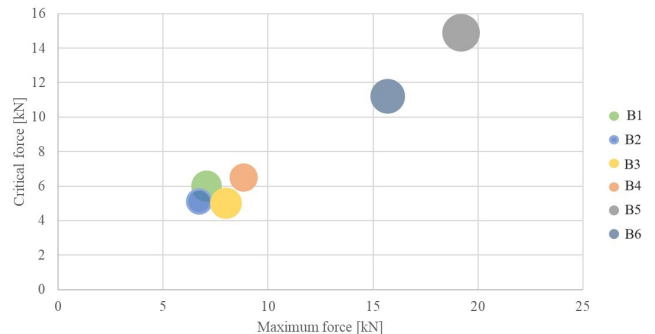

Fig. 14. Correlation of maximum and critical forces with beams weight

In summary, perforations in beams with modified cross-sections reduce both critical and maximum force values while lowering the section's weight. Designers must consider whether the weight reduction justifies the decrease in force capacity. In practice, these findings suggest that when weight reduction is prioritized, especially in applications such as aerospace or automotive engineering, the balance between weight savings and stability losses must be carefully evaluated.

Beams B3 and B4 showed higher critical and maximum forces for the perforated beam (B4) despite a 9% weight reduction. However, geometric imperfections might affect these force values.

Figure 15 illustrates the geometric imperfections in beams B1, B3, and B5. The yellow colour represents the ideal CAD dimensions, while black shows deviations projected onto the
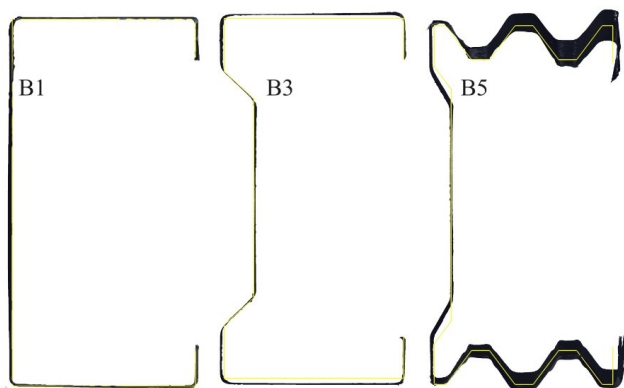
8

Bull. Pol. Acad. Sci. Tech. Sci., vol. 73, no. 3, p. e153830, 2025

Fig. 15. Geometric imperfections of the cross sections of the beams

cross-sectional view of the beam along its entire length. Beam B5 exhibits the greatest deviations. This suggests that even small geometric imperfections, especially in thin-walled beams, can substantially impact strength and stability. These geometric imperfections significantly impact the strength and stability of thin-walled beams with modified cross-sections, a key focus of the authors' ongoing research. Figure 15 illustrates geometric imperfections in channel profiles with a solid, flat web. It is important to note that the perforation of the web may have generated larger geometric imperfections than those observed for channels with a solid, flat web, which could have directly influenced the obtained results.

6. SUMMARY

The results of the experimental and numerical analyses highlight the intricate relationships between beam design, perforations, and structural performance. The following conclusions summarize the key findings regarding the effects of perforations on beam characteristics and stability.

- Perforations in beams can reduce their weight but generally decrease load-bearing capacity and stability.
- In some cases, perforations improve stiffness and stress distribution, increasing load capacity.
- Local and distortional buckling is more pronounced in complex cross-sectional shapes.
- Geometric imperfections significantly affect the stability of thin-walled beams with perforations.
- In designing lightweight structures, it is crucial to balance weight reduction with maintaining adequate load capacity.

The key conclusions from the conducted research indicate that modifying the cross-sectional shape of the beam leads to an increase in its stiffness, strength, and resistance to loss of stability. Furthermore, perforation causes a slight reduction in strength and stability parameters compared to the decrease in weight.

In addition to the experimental tests and FSM analysis, numerical analyses using the finite element method (FEM) and analytical calculations were also conducted. The application of FEM allows for precise modelling and analysis of complex stress and strain states, which is particularly important for thin-walled

structures with modified cross-sectional shapes. Analytical calculations provide a complementary approach, offering a theoretical basis for understanding the behaviour of these structures under various loading conditions. These methods are essential for capturing nonlinear behaviours, especially in perforated structures, which experience complex stress distributions.

This study had several limitations, including a focus on short beams due to the availability of suitable testing machines. The geometry of the perforations was constrained by the production capabilities of the collaborating company. Failure mechanisms were not analyzed, which remains an important direction for future research. Additionally, the higher production cost of modified cross-sections and the need for broader market promotion present further challenges.

To ensure clarity and avoid overwhelming the reader with excessive detail, the entire research program has been divided into two articles. This division prevents the article from becoming overly lengthy and disorganized, making the content more accessible and easier to follow for the reader. The results of the FEM and analytical analyses will be presented in the second part of this publication.

REFERENCES

[1] A.M. Pawlak, T. Górny, Ł. Dopierała, and P. Paczos, "The Use of CFRP for Structural Reinforcement – Literature Review," *Metals (Basel)*, vol. 12, no. 9, p. 1470, Sep. 2022, doi: 10.3390/met12091470.

[2] P. Paczos and A.M. Pawlak, "Experimental optical testing and numerical verification by CuFSM of compression columns with modified channel sections," *Materials*, vol. 14, no. 5, p. 1271, 2021, doi: 10.3390/ma14051271.

[3] A. Shahbazian and Y.C. Wang, "Direct Strength Method for calculating distortional buckling capacity of cold-formed thin-walled steel columns with uniform and non-uniform elevated temperatures," *Thin-Walled Struct.*, vol. 53, pp. 188–199, 2012, doi: 10.1016/j.tws.2012.01.006.

[4] Q.Y. Li and B. Young, "Structural performance of cold-formed steel built-up section beams under non-uniform bending," *J. Constr. Steel Res.*, vol. 189, p. 107050, 2022, doi: 10.1016/j.jcsr.2021.107050.

[5] P. Zhang and M.S. Alam, "Compression tests of thin-walled cold-formed steel columns with Σ-shaped sections and patterned per-

Bull. Pol. Acad. Sci. Tech. Sci., vol. 73, no. 3, p. e153830, 2025

9

P. Paczos, A.M. Pawlak, P. Jasion, and M. Plust

forations distributed along the length," *Thin-Walled Struct.*, vol. 174, p. 109082, 2022, doi: 10.1016/j.tws.2022.109082.

[6] M. Obst, M. Rodak, and P. Paczos, "Limit load of Cold formed thin-walled nonstandard channel beams," *J. Theor. Appl. Mech. (Poland)*, vol. 54, no. 4, pp. 1369–1377, 2016, doi: 10.15632/jtam-pl.54.4.1369.

[7] E. Magnucka-Blandzi, P. Paczos, and P. Wasilewicz, "Buckling study of thin-walled channel beams with double-box flanges in pure bending," *Strain*, vol. 48, no. 4, pp. 317–325, 2012, doi: 10.1111/j.1475-1305.2011.00825.x.

[8] M.T. Chen, B. Young, A.D. Martins, D. Camotim, and P.B. Dinis, "Experimental investigation on cold-formed steel lipped channel beams affected by local-distortional interaction under non-uniform bending," *Thin-Walled Struct.*, vol. 161, p. 107494, 2021, doi: 10.1016/j.tws.2021.107494.

[9] X. Yao, "EWM-based design method for distortional buckling of cold-formed thin-walled lipped channel sections with holes," *Math. Bio. Eng.*, vol. 19, no. 1, pp. 972–996, 2022, doi: 10.3934/mbe.2022045.

[10] G.C. de Salles, E. de M. Batista, and D.C.T. Cardoso, "Explicit equations for anti-symmetric distortional buckling of thin-walled lipped channel columns," *Thin-Walled Struct.*, vol. 176, p. 109325, 2022, doi: 10.1016/j.tws.2022.109325.

[11] X. Yao, J. Yang, and Y. Guo, "Study on Restoring Force Model of Cold-Formed Thin-Walled Steel Lipped Channel Beam-Columns under Cyclic Load," *Buildings*, vol. 13, no. 1, p. 114, 2023, doi: 10.3390/buildings13010114.

[12] D. Akchurin, C. Ding, Y. Xia, H.B. Blum, B.W. Schafer, and Z. Li, "Instability-driven family optimization of cold-formed steel lipped-channel cross-sections with strength and stiffness constraints," *Thin-Walled Struct.*, vol. 192, p. 111118, 2023, doi: 10.1016/j.tws.2023.111118.

[13] D.S. Khazaal, H.M. AL-Khafaji, and I.A. Abdulsahib, "Parametric Study on Buckling Behavior of Aluminum Alloy Thin-Walled Lipped Channel Beam with Perforations Subjected to Combined Loading," *Eng. Technol. J.*, vol. 39, no. 1A, pp. 89–103, 2021, doi: 10.30684/etj.v39i1a.1710.

[14] N.T. Yu, X.H. Huang, X.H. Xu, Z.M. Chen, and W. Bin Yuan, "An Analytical Solution for Lateral-Torsional Buckling Resistance of Perforated Cold-Formed Steel Channel Beams with Circular Holes in Web," *Int. J. Struct. Stab. Dyn.*, vol. 22, no. 16, p. 2250188, 2022, doi: 10.1142/S0219455422501887.

[15] J.S. Rajkannu and S.A. Jayachandran, "Flexural-torsional buckling strength of thin-walled channel sections with warping restraint," *J. Constr. Steel Res.*, vol. 169, p. 106041, 2020, doi: 10.1016/j.jcsr.2020.106041.

[16] H. Muteb and N. Alshareef, "Lateral-torsional buckling of thin-waaled sheet used as cold-formed beam," *Iraqi J. Mech. Mater. Eng.*, vol. 22, no. 4, 2023. doi: 10.13140/RG.2.2.10432.51208.

[17] D. Visy, M. Szedlák, B.B. Geleji, and S. Ádány, "Flexural buckling of thin-walled lipped channel columns with slotted webs: Numerical and analytical studies," *Eng. Struct.*, vol. 197, p. 109399, 2019, doi: 10.1016/j.engstruct.2019.109399.

[18] L. Wang, M. Hu, and B. Young, "Tests of aluminum alloy perforated built-up sections subjected to bending," *Thin-Walled Struct.*, vol. 158, p. 107136, 2021, doi: 10.1016/j.tws.2020.107136.

[19] N. Ting Yu, B. Kim, L. Yuan Li, W. Jian Hong, and W. Bin Yuan, "Distortional buckling of perforated cold-formed steel beams subject to uniformly distributed transverse loads," *Thin-Walled Struct.*, vol. 148, p. 106569, 2020, doi: 10.1016/j.tws.2019.106569.

[20] J. Kasprzak and P. Paczos, "Numerical and experimental validation of a test stand of cold-formed thin-walled beams," *Modelowanie Inżynierskie*, vol. 11, no. 42, pp. 209–216, 2011.

[21] X.H. Huang, L. Bai, J. Yang, F.L. Wang, J. Zhu, and Q.F. Liu, "Distortional-buckling analysis of channel sections with web stiffened by longitudinal ribs subjected to axial compression or bending," *Thin-Walled Struct.*, vol. 144, p. 106322, 2019, doi: 10.1016/j.tws.2019.106322.

[22] M. Grenda and P. Paczos, "Experimental and numerical study of local stability of non-standard thin-walled channel beams," *J. Theor. Appl. Mech. (Poland)*, vol. 57, no. 3, pp. 549–562, 2019, doi: 10.15632/jtam-pl/109601.

[23] C. Szymczak and M. Kujawa, "Buckling and initial post-local buckling behaviour of cold-formed channel member flange," *Thin-Walled Struct.*, vol. 137, pp. 177–184, 2019, doi: 10.1016/j.tws.2019.01.011.

[24] Y. Zhang, and X. Zhuang, "Cracking elements: A self-propagating Strong Discontinuity embedded Approach for quasi-brittle fracture," *Finite Elem. Anal. Des.*, vol. 144, pp. 84–100, 2018, doi: 10.1016/j.finel.2017.10.007.

[25] N.H. Abu-Hamdeh, K. Daqrouq, and F. Mebarek-Oudina, "Simulation and Analysis with Wavelet Transform Technique and the Vibration Characteristics for Early Revealing of Cracks in Structures," *Math. Probl. Eng.*, vol. 2021, p. 6626232, 2021, doi: 10.1155/2021/6626232.

[26] Y. Zhang, J. Huang, Y. Yuan, and H.A. Mang, "Cracking elements method with a dissipation-based arc-length approach," *Finite Elem. Anal. Des.*, vol. 195, p. 103573, 2021, doi: 10.1016/j.finel.2021.103573.

[27] http://zaprom.pl/fundusze-ue/